Evaluation of Gas Chromatography Columns with Radially Elongated Pillars as Second-Dimension Columns in Comprehensive Two-Dimensional Gas Chromatography

Meziani, Amel; Verloy, Sandrien; Ferroukhi, Ouassila; Roca, Sebastien; Curat, Aurelien; Tisse, Severine; Peulon-Agasse, Valerie; Gardeniers, Han; Desmet, Gert; Cardinael, Pascal

Published in:
Analytical Chemistry

DOI:
10.1021/acs.analchem.2c01264

Publication date:
2022

Document Version:
Accepted author manuscript

Evaluation of GC columns with radially-elongated pillars as second dimension columns in comprehensive two-dimensional gas chromatography (GC×μGC)

Amel Meziani[*, ¥], Sandrien Verloy[†, §], Ouassila Ferroukhi[¥], Sebastien Roca[*], Aurelien Curat[*], Severine Tisse[*], Valerie Peulon-Agasse[*], Han Gardeniers[§], Gert Desmet[†] and Pascal Cardinael[*].

[*]Laboratoire SMS UR3233, UNIROUEN, FR CNRS 3038, Place Emile Blondel, F-76821, Mont-Saint-Aignan, France.

[¥]Laboratoire de Chromatographie, Faculté de Chimie, USTHB, BP 32 EL-Alia, Alger, 16111 Algeria.

[†]Department of Chemical Engineering CHIS, Vrije Universiteit Brussel, Brussels 1050, Belgium.

[§]Mesoscale Chemical Systems, University of Twente, Enschede, 7522, NB, Netherlands.

ABSTRACT: The present study investigated the use of a dedicated GC column (*L*= 70 cm, 75 μm deep and 6.195 mm wide) with radially-elongated pillars (REPs) as the second column in comprehensive two-dimensional gas chromatography system (GC×μGC). Three stationary phases (apolar polydimethylsiloxane (PDMS), medium polar room temperature ionic liquid (RTIL) based on monocationic phosphonium and polar polyethylene glycol (PEG-1000)) have been coated using the static method at constant pressure or using an original vacuum pressure program from 400 mbar to 4 mbar. The best efficiency reached up to N = 62,000 theoretical plates for a film thickness of 47 nm at 100 °C for an *iso*-octane peak (k=0.16) at an optimal flow rate of 4.8 mL/min. The use of the vacuum pressure program improved the efficiency by approximately 15%. Efficiencies up to 28,000 and 47,000 were obtained for PEG-1000 and RTIL, respectively. A temperature-programed separation of a mixture of 11 volatile compounds on a PDMS-coated chip was obtained in less than 36 s. The PDMS-, PEG-1000- and RTIL-coated chips were tested as the second column using a microfluidic reverse fill/flush flow modulator in a GC×μGC system. The REP columns were highly compatible with the operating conditions in terms of flow rate and with more than 30,000 plates for the *iso*-octane peak. Moreover, a commercial solvent called *white spirit* containing alkanes and aromatic compounds was injected on three sets of columns in normal and reverse modes, demonstrating the great potential of the chip as a second dimension separation column.

The miniaturization of analytical systems has been the center of interest over the past decades to resolve the needs of new technologies such as space exploration, drug analysis and field applications. [1] The first microanalytical device made was a gas chromatograph on a chip, which was introduced by Terry et al. in 1979. [2] Since then, a significant growth in GC chip research has been supported[3] by the development of microelectromechanical system (MEMS) technology. Several chip designs have been studied, and the most common geometries are serpentine, circular spiral and square spiral. [4] The channel cross-section geometries can be rectangular, square, trapezoidal or semicircular.[5] In 2009, Ali et al.[6] and Nakai et al.[7] introduced a new geometry, called pillar array columns (PACs), by incorporating pillar arrays in the channel; this provided an increase in sample capacity and improved efficiency.[1] Recently, Jespers et al.[8] developed PACs with radially elongated pillars (REPs). The latter are stretched out in the direction perpendicular to the flow. The chip is designed as a serpentine channel with a length of 70 cm divided into 10 segments connected by turns.[8] Each segment has a width of 6.195 mm and is filled with a grid of pillars, with an interpillar distance of 75 μm, creating 8 parallel flow paths.[9] The REP design has advantages over circular pillars because of the important decrease in the effective axial diffusion proportionally to the square (very high) flow-through path tortuosity that they induce.[10] Moreover, the sidewall-induced dispersion can be practically completely suppressed due to the reduced difference in the flow resistance between the flow-through channels near the sidewalls and the rest of the bed.[11]

The main challenge that most of the previous studies were confronted with was obtaining a uniform coating of the stationary phase on chips. This is due to the multiple turns and the noncylindrical geometry that makes it difficult to maintain the uniformity of the stationary phase in the channel.[12] The stationary phase coating methods mostly used were the same as those for capillary columns, which were dynamic or static methods. The dynamic method has been used in a number of reports[13–15] because the procedure is simple and fast. However, a low film quality was frequently obtained, and the impossibility of predicting the film thickness[16] further reduced the interest in this method. The static method remains the most used method because it is known to provide reproducible and good efficiencies, and the film thickness can be easily controlled and predicted.[17] Unfortunately, the major problem with the static method in the case of chip coating is the formation of gas bubbles during the

filling process or when the chip is placed under vacuum.[1] The latter could be attributed to cavitation due to microcavities on the channel surface or the external chip interfaces where the gas bubbles can be generated.[18] The simplest solution to avoid this problem is to pressurize the filled chip before applying vacuum[19] to dissolve gas bubbles.

The use of various stationary phases for chip coatings has been reported.[3] For nonpolar stationary phases, polydimethylsiloxane has been the most frequently used, given its high thermal stability, chemical inertness and broad range of operating temperatures.[20] To extend the range of applications, other stationary phases have been used and were reported by Azzouz et al.[21] The use of room-temperature ionic liquid (RTIL) for chip coating has been investigated by several authors.[22,23] Regmi et al.[24] succeeded in separating a mixture of 15 pollutants with symmetrical peaks. Furthermore, Colin et al.[25] used a chip coated with trigonal tricationic RTIL as a second column of a comprehensive two-dimensional gas chromatographic system with microfabricated components (μGC×μGC).

Conventional comprehensive two-dimensional GC (GC×GC) has been, until now, the most effective method for the separation of complex mixtures of volatile and semivolatile compounds.[26] The compounds are preseparated in a long first dimension column and then reinjected into a shorter second dimension column coated with a stationary phase of different polarity. The main advantage of GC×GC is that it provides higher peak capacities[27], thus offering a higher resolution and detectability compared to a conventional GC system. The modulator between the two columns could be either a thermal modulator[26] or a flow modulator.[28] The main advantages of the flow modulators compared to thermal ones are the lower operational cost and their simplicity of use.[28] Two flow modulators are available depending on the pathway flows, the forward flush/fill (FFF) modulator and the reverse fill/flush (RFF) flow modulator. The internal diameter of the second column is larger than the internal diameter of the first column to limit the effect of the reinjected volume. The RFF modulator in principle allows enhanced resolution, thanks to a shorter injection pulse when the sample loop is partially filled. Nevertheless, flow modulators suffer from some drawbacks due to the high flow rate in the second column, which limits the use of a mass spectrometer as a detector. In addition, the linear velocity is far from the optimum velocity; thus, the length should be sufficient to compensate for the loss of efficiency. Moreover, the reinjected volume in the second column needs to be limited compared to the volume of the second column and its capacity. The use of REP columns could resolve these drawbacks thanks to their large volume and high capacity as well as their short length, allowing a short retention time.

In the present study, REP columns were coated with several stationary phases, including apolar PDMS, medium polar RTIL based on monocationic phosphonium derivative and polar PEG-1000. The static method was used for all the coatings, and a sol-gel process was used for the preparation of RTIL and PEG-1000. The solvent evaporation step was performed using a fixed vacuum pressure and vacuum pressure program to compare its influence on the coating homogeneity. The column efficiencies were evaluated and compared to the efficiency of the uncoated chip for the injection of *iso*-octane at 100 °C. Van Deemter plots were established, and the A, B and C terms and the optimal gas linear velocity were determined. A mixture of volatile organic compounds was injected on a PDMS-coated chip using a temperature program to evaluate the chip performances.

For the first time, REP columns coated with PDMS, PEG-1000 and RTIL were used in a GC×μGC system as the second dimension column. Although the technology of the second column is based on micro-technology, the system developed is not intended to be miniaturized Both the normal and reverse modes were explored. A microfluidic RFF modulator was used with a capillary column of 100 μm i.d. in the first dimension. The separation of a mixture of alkanes and aromatic compounds (commercial white spirit) was performed and evaluated.

EXPERIMENTAL SECTION

Chemicals. 1,1,1,3,3,3-hexamethyldisilazane (HMDS), methyltriethoxysilane (MTEOS), 2,2,4-trimethylpentane (*iso*-octane), 4-methyl-2-pentanone, isobutyl acetate and butyl acetate were purchased from Acros Organics (Morris Plains, New Jersey, USA). Pentane, dichloromethane and trichloroethylene were obtained from VWR International (West Chester, USA). Octane was purchased from Janssen Chemica (Geel, Belgium). Polyethylene glycol (PEG-1000) and hexan-2-one were obtained from Sigma–Aldrich (St. Louis, Missouri, USA). Chlorobenzene was purchased from Prolabo (Rhône-Poulenc, France). Toluene was obtained from Honeywell (Morris-Plains, New Jersey, USA). Propanol was purchased from Fisher Chemical (Waltham, Massachusetts, USA). PDMS OV-1 was purchased from MEGA (Legnano, Italy). Butanone was purchased from Fluka (Steinheim, Germany). White Spirit (Mieuxa) was purchased from Leroy Merlin (Isneauville, France).

Chip coating. The REP columns were designed as a serpentine channel with a total length of 70 cm, consisting of 10 segments of 6.195 mm wide. Each channel was filled with a grid of pillars with a width of 1.4 mm spaced 75 μm apart in the axial direction[8]. Connections were made using two fused silica capillaries of 250 μm i.d. and a NanoPort assembly.

Pretreatment processes were employed before coating the REP columns. For the PDMS coating, silanization of the chip surface was performed prior to coating. The chip was then placed at 100 °C in a gas chromatograph oven, and a silanization reagent (HMDS) was pushed through the chip at 0.1 mL/h using a syringe pump model NE-100 Multi-PhaserTM (WPI, Montluçon, France) and set for 6 h. After this step, the chip was washed with methanol and then diethyl ether for 30 min each using Western Fluids Engineering SP-400 Nanobaume (Wildomar, CA, USA). REP columns were dried under nitrogen flow for 2 h. A static method was used for chip coating. First, a solution of 3 mg/mL of PDMS was prepared in a mixture of pentane/DCM (50/50, v/v), subsequently filtered (polytetrafluoroethylene 0.45 μm) and sonicated for 30 min. Afterward, the chip was filled with the PDMS solution using the Nanobaume. When all gas bubbles were evacuated from the chip, the outlet was sealed and pressurized for 3 h. The inlet of the chip was connected to a vacuum pump model SC920 (KNF Lab, Aartselaar, Belgium) at a controlled pressure until complete evaporation of the solvent. For the final step, the chip was heated from 40 °C to 100 °C at 1 °C/min for 6 h under helium. The same method

was performed with a solution of 2 mg/mL of PDMS to produce a thinner film.

Polar stationary phases were prepared using a sol-gel process.[29] The sol-gel process involves two main reactions, first the hydrolysis of the silylated alkoxide and then the polycondensation of the formed silanol groups. A mass of 100 mg of the polymer (PEG-1000) was dissolved in 500 µL of a solvent (DCM). Subsequently, 200 µL of a precursor (MTEOS) and 200 µL of a catalyst (TFA) containing 5% of water were added. The mixture was thoroughly mixed and stirred for 4 h. The solution was evaporated under nitrogen at room temperature. The obtained xerogel (sol-gel PEG-1000) was used to prepare the sol-gel stationary phase solution. A mass of 30 mg of sol-gel PEG-1000 was dissolved in 20 mL of pentane/DCM mixture (50/50, v/v). The coating of the chip was performed as previously described using the static method. Another sol-gel coating was performed using RTIL, tributyl[3-(triethoxysilyl)propyl(phosphonium)] chloride (Figure 1).

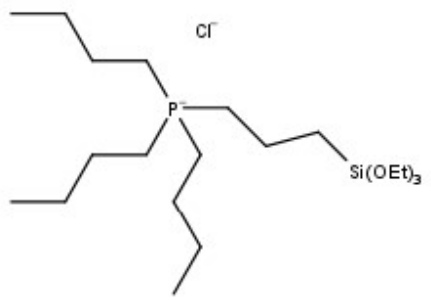

Figure 1. Chemical structure of the RTIL used for the chip coating

To evaluate the coating film homogeneity, microscope images were obtained with a Nikon Eclipse LV100 microscope (maximum magnification: 1000×) coupled to a CCD camera connected to a computer. The data acquisition was performed via NIS-Elements D software (version 3.1).

Efficiency measurements. For efficiency evaluation, the manifold was equipped with deactivated fused silica capillaries of approximately 30 cm lengths and 250 µm i.d. for the inlet, 100 µm i.d. for the outlet to ensure connections with the injector and the detector, respectively.

A volume of 0.1 µL of *iso*-octane vapor was injected under isothermal temperature at 100 °C using an Agilent 7890B gas chromatograph with a flame ionization detector (FID) and an Agilent G4513A autosampler. Agilent OpenLAB CDS ChemStation Edition (Rev.C.01.05.2013) software was used for data acquisition and data processing. The internal diameter of the insert was chosen at 1.2 mm (length 8 cm) to minimize its volume. The temperatures of the injector and detector were set at 200 °C and 180 °C, respectively. The nitrogen, hydrogen and air flows of the detector were maintained at 10, 30 and 300 mL/min, respectively. Hydrogen was chosen as the carrier gas due to its low viscosity. The split flow was maintained at 100 mL/min, and the pressure was set from 50 kPa to 500 kPa. To calculate the column's plate number, the average of three measurements of the retention time and the width at half height was calculated.

GC×µGC analyses. Analyses were performed using three sets of columns. In reverse mode, equity 1701 (13 m × 100 µm × 0.1 µm) was used as the first column with a flow rate of 0.15 mL/min, and a chip coated with PDMS was used as the second column with a flow rate of 4 mL/min. Another two sets of columns for normal mode consisted of an equity™-1 (14 m × 100 µm × 0.1 µm) with a flow rate of 0.20 mL/min as the first column and a PEG-1000-coated chip with a flow rate of 6.40 mL/min as the second column and an equity™-1 (12 m × 100 µm × 0.1 µm) with a flow rate of 0.10 mL/min as the first column and an RTIL-coated chip with a flow rate of 6.80 mL/min as the second column. The chosen internal diameter of the connected capillaries was fixed at 250 µm i.d. to limit the pressure drop for its use in GC×µGC. A microfluidic RFF modulator was used. After optimization using a homemade Excel datasheet[30], the injection time and modulation period were set to 0.12 s and 5 s, respectively. A bleed capillary with an i.d. of 50 µm and a length of 5 m was connected between the modulator and a thermal conductivity detector. The following temperature program was used: 50 °C (2 min) ramp up at 7 °C/min to 150 °C with a hold time of 2 min. First, a volume of 0.1 µL of white spirit (a mixture of alkanes and aromatic compounds) was injected. After that a sample of commercial gasoline SP95 was analyzed under the same conditions in the reverse mode.

RESULTS AND DISCUSSION

Coating evaluation. Considering that the solution concentration and the volumetric mass density of the stationary phases are equal to 1000 g/L, the film thicknesses can be estimated at 47 nm and 71 nm for the PDMS coatings and at 71 nm and 47 nm for PEG-1000 and RTIL, respectively.

The evaporation process is the crucial step to obtain film homogeneity using a static coating method. Throughout the filling and evaporation steps, it is important to avoid the formation of gas bubbles. After sealing, the chip was maintained under pressure for at least 2 h to dissolve gas microbubbles. However, the chip must also be manipulated meticulously to prevent gas bubble formation in the junction between the outlet and the capillary. The visual evaluation of the solvent-evaporation process, with a constant vacuum pressure (CVP), showed that the velocity of the evaporation in the first channel segment was very fast (approximately 30 s) compared to the rest of the column segments (2 h for the complete evaporation of the solvent from the chip), which led to an irregular coating. This was confirmed by the microscope images (Fig. 2 *a*), where some defects were observed, especially on the glass cover surface.

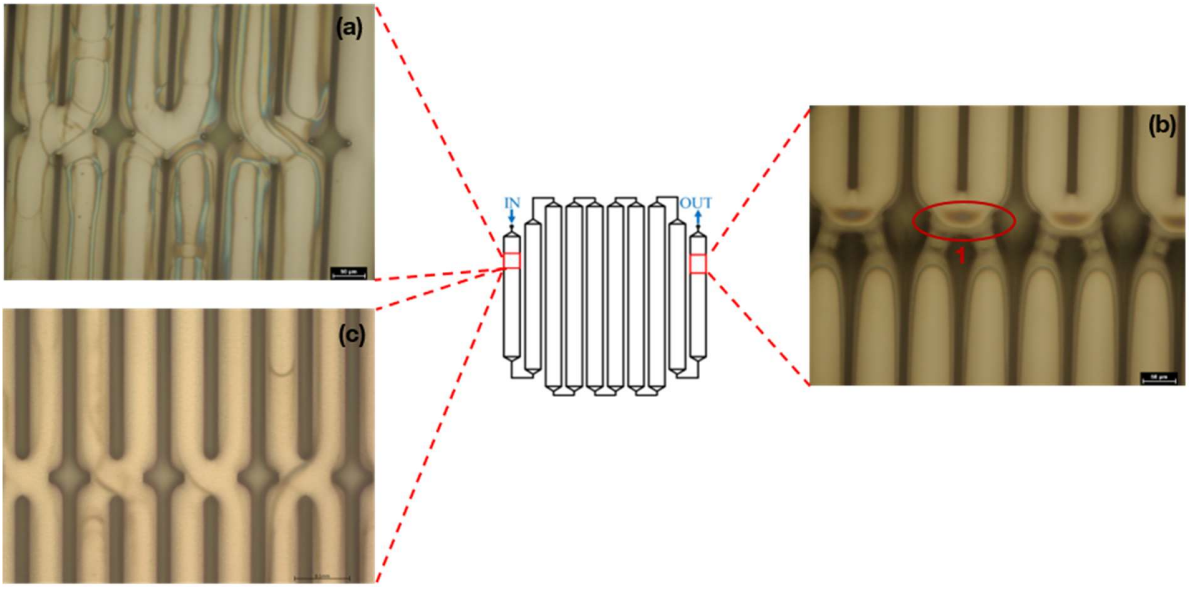

Figure 2. Optical microscopy images (taken from the top) of the VPP and CVP PDMS coatings at different locations: (*a)* first segment of the chip using CVP, *(b)* segment showing stationary phase pooling (red ellipse 1) in the right-angled corners using CVP, *(c)* first segment of the chip using VPP

The evaporation appeared uniform for the rest of the segments; however, the microscope images showed that the stationary phase accumulated in the corners of the channel (Fig. 2 *b (1)*). To overcome this problem, a vacuum pressure program (VPP) from 400 mbar to 4 bar was used during the coating evaporation step to homogenize the evaporation rate, and a significant improvement of the coating was observed (Fig. 2 *c*); nevertheless, the slowdown of the evaporation rate led to the same stationary phase pooling for the last segments of the chip.

Evaluation of efficiency. The column efficiency (theoretical plate number *N*) was evaluated by injection of *iso*-octane in triplicate. Figure 3 shows an overview of the different Van Deemter curves obtained for different coated REP columns, plotting the observed height equivalent to one theoretical plate (HETP) as a function of the velocity of the gas. As can be noted, a minimal plate height of 11 µm is obtained at approximately 12 cm/s for *iso*-octane ($k = 0.16$) with the 47 nm PDMS coating corresponding to 62,000 theoretical plates (represented by ●). Compared to an uncoated chip (75,000 theoretical plates), a significant loss of the number of plates is noticed, as already observed by Jespers et al.[8] The efficiency measured here is similar to that obtained by Jespers et al.[8], with approximately 60,000 for the same compound at 100 °C.

For the PDMS-coated chip with a film thickness of 71 nm using VPP (●), a minimal plate height of 16 µm was obtained, corresponding to 44,000 theoretical plates. However, the coated chip with the same film thickness using a CVP (●) showed a lower number of theoretical plates corresponding to 38,000. These results confirm the improvement of film homogeneity using VPP compared to the use of CVP. As expected, we notice that the plate number increases when the film layer is thinner. Concerning the polar coatings, the chip coated with the RTIL (represented by▲) showed a better efficiency than the chip coated with PEG-1000 (▲) with minimal plate heights of 15 µm at 100 °C and 25 µm at 80 °C. The temperature was set at 80 °C for PEG-1000 to have a higher retention with *iso*-octane.

The optimum pressure was approximately 300 kPa, whatever the stationary phase. The corresponding optimum flow rate and velocity are 4.8 mL/min and 12 cm/s, respectively. The velocity appeared to be lower than the value obtained with a conventional capillary column (40 cm/s). However, the high optimum flow rate implies that the REP columns are very well suited for use as a second column in GC×µGC and are compatible with mass spectrometry detection.

The terms A, B and C of the Van Deemter equation have been deduced from the experimental values and are shown in Table 1. In agreement with the theory, the A-terms (eddy diffusion) were equal to zero for all the coated REP columns. The B-term is completely dependent on the solute diffusivity in the gas. For all coatings, the B-term values were approximately 1.40×10^{-2} cm^2/s except for the chip coated with PEG-1000, where the temperature was set at 80 °C.

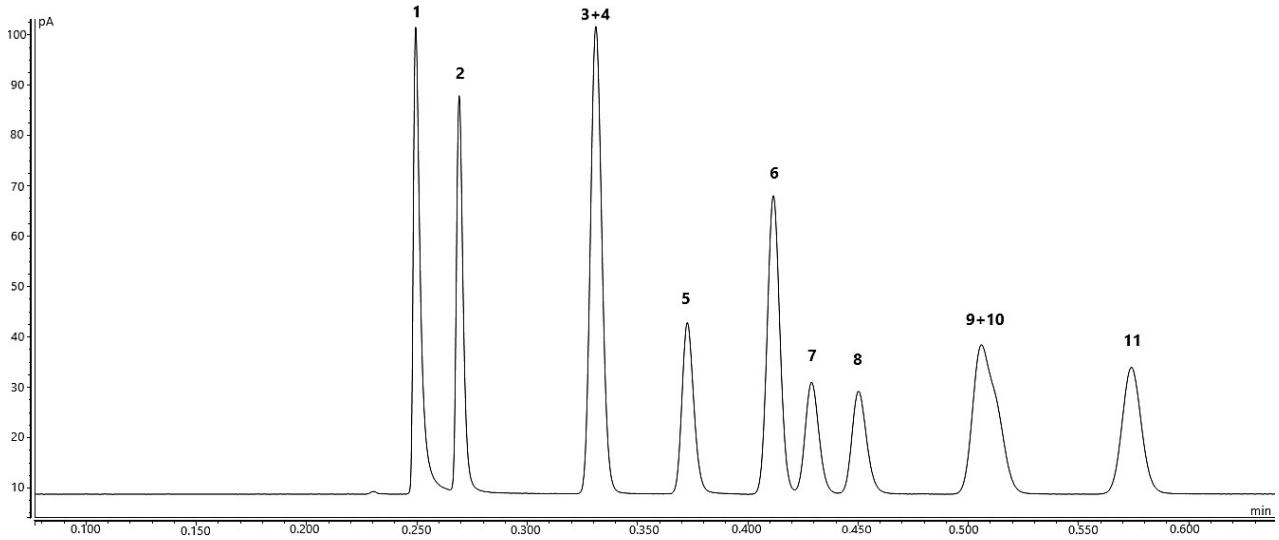

Figure 4. Temperature-programmed separation of a mixture of 11 compounds on the PDMS-coated chip: (1) 1-propanol (N = 34 356), (2) 2-butanone (N = 39 3664), (3) trichloroethylene, (4) *iso*-octane (5) 4-methyl-2-pentanone (N = 23 285), (6) toluene (N = 24 366), (7) isobutyl acetate (N = 22 163), (8) 2-hexanone (N = 21 835), (9) octane, (10) butyl acetate, and (11) chlorobenzene (N = 20 118). T_{oven}, 40-80 °C at 10 °C/min

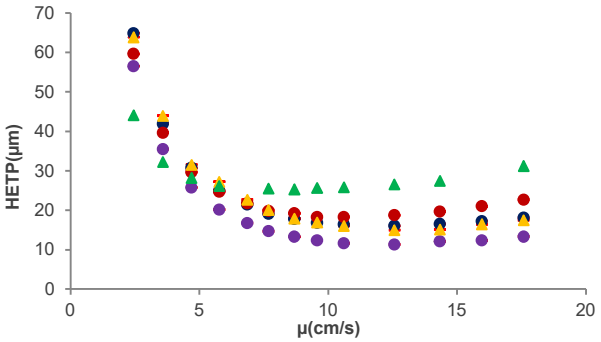

Figure 3. HETP as a function of the gas linear velocity obtained for the injection of *iso*-octane at 100 °C except for PEG-1000 at 80 °C, µ was calculated by the injection of methane at the same temperature ● 47 nm PDMS coating using CVP, ● 71 nm PDMS coating using VPP, ● 71 nm PDMS coating using CVP, ▲ 47 nm RTIL coating using CVP, ▲ 71 nm PEG-1000 coating using CVP

Concerning C-terms, a lower value was observed for the PDMS coating of 71 nm using the VPP (4 $\times 10^{-2}$ s) than the value obtained with the PDMS coating of 71 nm using CVP (5.9 $\times 10^{-2}$ s). This could be attributed to the defects in the coating using a CVP, leading to poor homogeneity of the film thickness in the first segment of the chip. For the PDMS coating with a thinner film thickness (47 nm), the C- term was much lower (2 $\times 10^{-2}$ s). The values obtained for the polar coatings were higher compared to the PDMS coating, even twofold for the RTIL coating (4.1$\times 10^{-5}$ s) and more than 3-fold for the PEG-1000 coating (14 $\times 10^{-5}$ s).

Table 1. Van Deemter coefficients for the different coated REP columns obtained by fitting the experimental values with H=A+B/u+C.u

	PDMS 47 nm	PDMS VPP 71 nm	PDMS CVP 71 nm	PEG-1000* 71 nm	RTIL 47 nm
A (cm)	0.00	0.00	0.00	0.00	0.00
B×10^{-2} (cm^2/s)	1.40	1.43	1.43	1.00	1.45
C×10^{-5} (s)	2.00	4.00	5.90	14.0	4.10

*80 °C

^{1}D GC separation. A mixture of 11 volatile compounds with various functional groups and different boiling points was prepared and separated on a PDMS-coated chip. The pressure was maintained at 250 kPa, and the temperature program was set from 40 °C and ramped up to 80 °C at a rate of 10 °C/min.

Peaks were identified by injecting each compound individually and were labeled with corresponding compound numbers (Table 2). The chromatogram in Fig. 4 shows that 9 out of 11 peaks were well separated in less than 36 s, and most of them were clearly symmetrical. Peak symmetry factors are superior to 1 and below 1.3 for all separated peaks except for the most polar 1-propanol. However, trichlorethylene and iso-octane, octane and butyl acetate were not separated because the differences in boiling points were less than 1 °C. Therefore, these compounds cannot be well separated on a PDMS stationary phase.

Table 2. Peak number, retention times, asymmetries and boiling points of compounds included in the mixture injected on the PDMS-coated chip with a film thickness of 47 nm

	Compounds	t_R (min)	Peak symmetry (USP 10%)	b.p (°C)
1	1-propanol	0.249	1.82	97.5
2	2-butanone	0.269	1.29	80.1
3	Trichloroethylene	0.329	n.a	87.2
4	*Iso*-octane	0.331	n.a	99.3
5	4-methyl-2-pentanone	0.372	1.16	117.5
6	Toluene	0.412	1.07	110.6
7	Isobutyl acetate	0.429	1.10	118
8	2-hexanone	0.450	1.17	127.6
9	Octane	0.506	n.a	125.5
10	Butyl acetate	0.513	n.a	126
11	Chlorobenzene	0.574	1.07	131

^{2}D GC separation (GC×µGC). The columns used in the second dimension of a microfluidic GC×GC system should have some specific properties, which are very different from those used in thermal GC×GC systems. Moreover, the flow in the second column is totally independent of the first column flow and needs to be very high to completely and rapidly reinject the sample collected in the loop. Efficiency should remain high using a high flow, typically between 2-10 mL/min. However, these gas flows are not fully compatible with mass spectrometry, which prevents the spreading of the microfluidic GC×GC system. Some authors have proposed solutions to overcome this problem by using a Deans' switch generating short pulses at the cost of decreased sensitivity[31], a four-stage (low-flow modulation to reduce 2D flow[32] or a dynamic pressure gradient modulation technique. [33] REP column properties are promising due to their high volumetric loadability equivalent to those of 210 µm i.d. column and their high plate numbers achieved in a very short time, as presented in the first part of this article. The geometry of REP columns is particularly adapted in the second dimension because the efficiency remains high despite the high flow rate and the quantity of stationary phase limits the stationary phase overloading (fronting peak) allowing the injection of concentrated sample. It can be notice that the use of REP micro-columns in the first dimension of µGC×µGC system is not suitable because the flow rate of the first column must be low to limit the width of the reinjection band. To compare the performance of the REP column with a conventional column, efficiencies on an unretained compound were evaluated. The capillary column was chosen to have the same pressure drop as the REP column, allowing the use of the same bleed capillary and modulation conditions. The modulation times of the microfluidic RFF modulator were optimized using a homemade Excel datasheet[30] to elute the compounds at the optimal velocity in the chip. The filling time was set at 5 s, and the flushing time was 0.12 s. Under these conditions, the sample loop was filled at 9% and flushed at 10%, allowing complete reinjection of the collected sample. The retention times in the first and second columns and the peak efficiency measured for the injection of *iso*-octane are reported in Table 3.

Table 3. Retention time and efficiency measured for the injection of *iso*-octane at 80 °C, first column Equity 1701 (13 m×100 µm×0.1 µm)

Second column	^1t_R(min)	^2t_R(s)	^2N
REP column (0.7 m)	4.588	9.1	30,050
Capillary column (1.8 m×100 µm×0.1 µm)	4.458	1.4	1,130

^1t_R: retention time in the first dimension column

^2t_R: retention time in the second dimension column

^2N: plate number in the second dimension column

These results show that the REP column efficiency remained high, demonstrating that the reinjected volume did not overload the chip volume and that the linear velocity was close to the optimum. In contrast, the efficiency observed on the conventional capillary column (1,130) was far from the maximum theoretical value (18,000) (see the 2-D chromatograms of *iso*-octane in supporting information). The void time was estimated at 7.5 s on the REP column. However, the retention time in the REP column was higher than the modulation time, which led to the elution of *iso*-octane in the wrap around.

To demonstrate the interest of the REP column as the second column in the GC×µGC system, first a mixture of alkane and aromatic compounds was injected on three sets of columns in normal mode (apolar × polar) and reverse mode (polar × apolar). The temperature was programmed from 50 °C up to 150 °C at 7 °C/min. The maximum operating temperature of the chip was limited at 150 °C in isothermal conditions (170°C in temperature program) to avoid degradation of the ferrule assemblies. The chromatogram obtained for the reverse mode is presented in Fig. 6. It shows a good selectivity of the coated stationary phase, because all alkanes (the most retained compounds on the second column) are well separated from the aromatic compounds. The chromatograms in Figs. 7 and 8 represent the separation of the same mixture with two different sets of columns in normal mode (apolar × polar). The compounds are again well separated, and we noticed a reversal of the elution order; the alkanes were less retained in the second column. However, the void time is relatively long in the second dimension, which means that wrap around occurred to give broad modulated peaks. These results can be explained by the design of the pillar array columns with radially elongated pillars that are perpendicular to the flow. This special design provides a very high tortuosity of the flow, which makes the effective length of the channel 9 times larger than the nominal length[8] and gives more length for the analytes to be separated. An improvement could be to reduce the REP column length by 2 or 3 times, which can lead to more than 10,000 plates.

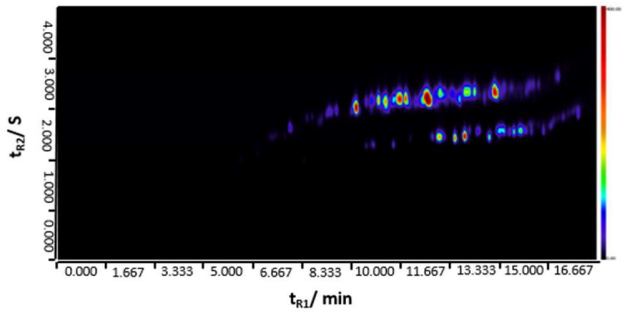

Figure 6. Contour 2-D chromatogram showing the separation of commercial *white spirit* with a capillary OV-1701 column in the 1st dimension and a PDMS-coated chip in the 2nd dimension

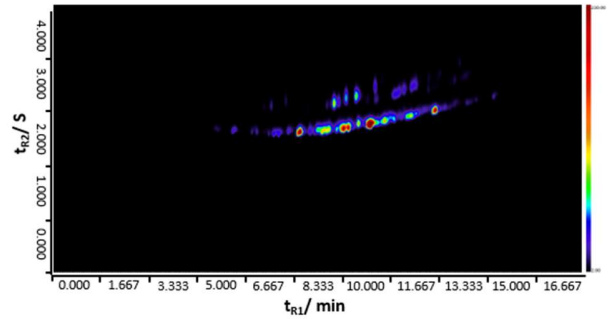

Figure 7. Contour 2-D chromatogram showing separation of commercial *white spirit* with capillary equity™-1 column in the 1st dimension and PEG-1000 coated chip in the 2nd dimension

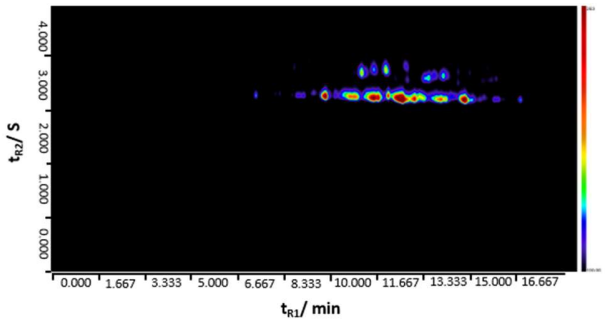

Figure 8. Contour 2-D chromatogram showing separation of commercial *white spirit* with capillary equity™-1 column in the 1st dimension and RTIL coated chip in the 2nd dimension

A lead-free gasoline 95 E5 which is a more complex sample was injected in the reverse mode. The chromatograms in Fig.9 a and Fig. 9 b showed the separation of the gasoline using a modulation time of 4 s and 6 s respectively. A good separation was observed with both conditions. Nevertheless, using a shorter modulation time peak efficiency in the first dimensionwas increased avoiding peak under-sampling.

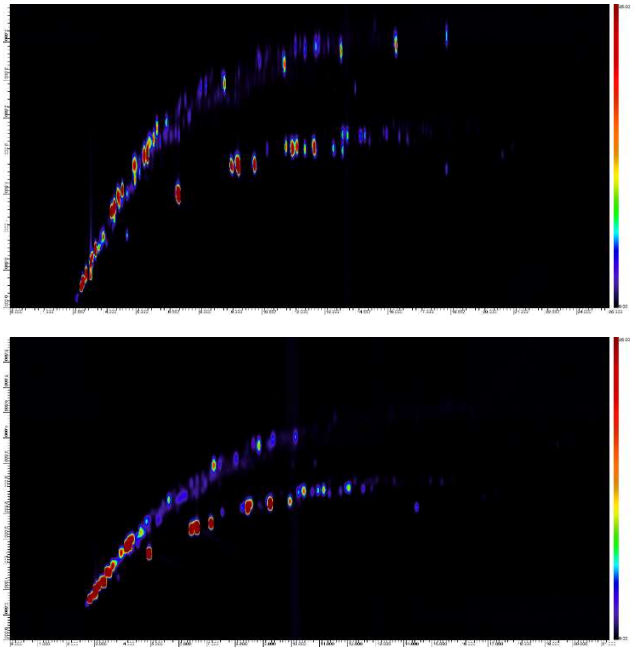

Figure 9. Contour 2-D chromatograms showing separation of commercial gasoline with a capillary OV-1701 column in the 1st dimension and a PDMS-coated chip in the 2nd dimension using 4s (*a*) and 6 s (*b*) as modulation time

CONCLUSION

In this study, the coating of five different REP columns was successfully realized. For the nonpolar stationary phase (PDMS), an efficiency up to *N*= 62,000 theoretical plates was obtained for a film thickness of 47 nm under isothermal conditions (100 °C) for an unretained compound (*iso*-octane). The use of a VPP for chip coating led to an improvement in the coating homogeneity (efficiency was increased by approximately 15%) compared to the coating using CVP.

The optimal flow rate was approximately 4.8 mL/min, reached at a pressure of 300 kPa corresponding to a velocity of 12 cm/s, which makes the REP columns compatible with mass spectrometry detection, which will be tested in a future study.

The analysis of a mixture of 11 components on a PDMS-coated chip was performed in less than 36 s with plate numbers between 39,366 and 20,118.

The performance of the REP column in the second dimension of a comprehensive GC×µGC system with an RFF modulator was evaluated by the injection of *iso*-octane. The efficiency remained high in the second dimension, which was allowed by the design of the REP column that was perfectly compatible with the generated flow of the RFF modulator. Moreover, the efficiency was more than 20 times higher than that of a capillary column, generating the same pressure drop. The mixture of alkanes and aromatic compounds was analyzed on three sets of columns in normal and reverse mode. Aromatic compounds were well separated from the alkanes on all three sets of columns. Nevertheless, the peaks obtained were slightly too wide, and the retention time was relatively long. Therefore, the system needs to be further

optimized, and shorter-length REP columns will be tested to reduce the dead time in the column and avoid wrap-around.

ASSOCIATED CONTENT

Supporting Information

2-D chromatograms of iso-octane using an REP column or a capillary column in the second dimension.

AUTHOR INFORMATION

Corresponding Author

*E-mail: pascal.cardinael@univ-rouen.fr

ORCID

Pascal Cardinael**: 0000-0001-8828-4527**

ACKNOWLEDGMENTS

A.M gratefully acknowledges the Partenariat Hubert Curien (PHC) Tassili 20MDU903 for its financial support (PhD grant A. M.).

REFERENCES

(1) Ghosh, A.; Vilorio, C. R.; Hawkins, A. R.; Lee, M. L. Microchip Gas Chromatography Columns, Interfacing and Performance. *Talanta* **2018**, *188*, 463–492. DOI : 10.1016/j.talanta.2018.04.088.

(2) Terry, S. C.; Jerman, J. H.; Angell, J. B. A Gas Chromatographic Air Analyzer Fabricated on a Silicon Wafer. *IEEE Trans. Electron Devices* **1979**, *26* (12), 1880–1886. DOI :10.1109/T-ED.1979.19791.

(3) Lussac, E.; Barattin, R.; Cardinael, P.; Agasse, V. Review on Micro-Gas Analyzer Systems: Feasibility, Separations and Applications. *Crit. Rev. Anal. Chem.* **2016**, *46* (6), 455–468. DOI :10.1080/10408347.2016.1150153.

(4) Radadia, A. D.; Salehi-Khojin, A.; Masel, R. I.; Shannon, M. A. The Effect of Microcolumn Geometry on the Performance of Micro-Gas Chromatography Columns for Chip Scale Gas Analyzers. *Sens. Actuators B Chem.* **2010**, *150* (1), 456–464. DOI :10.1016/j.snb.2010.07.002.

(5) Haghighi, F.; Talebpour, Z.; Sanati-Nezhad, A. Through the Years with On-a-Chip Gas Chromatography: A Review. *Lab. Chip* **2015**, *15* (12), 2559–2575. DOI :10.1039/C5LC00283D.

(6) Ali, S.; Ashraf-Khorassani, M.; Taylor, L. T.; Agah, M. MEMS-Based Semi-Packed Gas Chromatography Columns. *Sens. Actuators B Chem.* **2009**, *141* (1), 309–315. DOI :10.1016/j.snb.2009.06.022.

(7) Nakai, T.; Nishiyama, S.; Shuzo, M.; Delaunay, J.-J.; Yamada, I. Micro-Fabricated Semi-Packed Column for Gas Chromatography by Using Functionalized Parylene as a Stationary Phase. *J. Micromechanics Microengineering* **2009**, *19* (6), 065032. DOI :10.1088/0960-1317/19/6/065032.

(8) Jespers, S.; Schlautmann, S.; Gardeniers, H.; De Malsche, W.; Lynen, F.; Desmet, G. Chip-Based Multicapillary Column with Maximal Interconnectivity to Combine Maximum Efficiency and Maximum Loadability. *Anal. Chem.* **2017**, *89* (21), 11605–11613. DOI :10.1021/acs.analchem.7b03036.

(9) Jespers, S.; Lynen, F.; Desmet, G. Numerical Study and Theoretical Performance Limit of Interconnected Multi-Capillary Gas Chromatography Columns with Perfectly Ordered Pillar Patterns. *J. Chromatogr. A* **2017**, *1524*, 215–221. DOI :10.1016/j.chroma.2017.09.068.

(10) Callewaert, M.; Desmet, G.; Ottevaere, H.; De Malsche, W. Detailed Kinetic Performance Analysis of Micromachined Radially Elongated Pillar Array Columns for Liquid Chromatography. *J. Chromatogr. A* **2016**, *1433*, 75–84. DOI :10.1016/j.chroma.2015.12.086.

(11) Op De Beeck, J.; Callewaert, M.; Ottevaere, H.; Gardeniers, H.; Desmet, G.; De Malsche, W. Suppression of the Sidewall Effect in Pillar Array Columns with Radially Elongated Pillars. *J. Chromatogr. A* **2014**, *1367*, 118–122. DOI :10.1016/j.chroma.2014.09.052.

(12) de Mello, A. FOCUS. *Lab. Chip* **2002**, *2* (3), 48N. DOI :10.1039/b207266c.

(13) Lambertus, G.; Elstro, A.; Sensenig, K.; Potkay, J.; Agah, M.; Scheuering, S.; Wise, K.; Dorman, F.; Sacks, R. Design, Fabrication, and Evaluation of Microfabricated Columns for Gas Chromatography. *Anal. Chem.* **2004**, *76* (9), 2629–2637. DOI :10.1021/ac030367x.

(14) Yu, C M. High performance hand-held gas chromatograph. United States 1998.

(15) Wiranto, G.; Haskard, M. R.; Mulcahy, D. E.; Davey, D. E.; Dawes, E. F. Microengineered Open Tubular Columns for GC Analysis; Bergmann, N. W., Reinhold, O., Tien, N. C., Eds.; Gold Coast, Australia, 1999; pp 168–177. DOI :10.1117/12.364435.

(16) Grob, K. *Making and Manipulating Capillary Columns for Gas Chromatography*; Chromatographic methods; Hüthig: Heidelberg Basel New York, 1986.

(17) Bouche, J.; Verzele, M. A Static Coating Procedure for Glass Capillary Columns. *J. Chromatogr. Sci.* **1968**, *6* (10), 501–505. DOI :10.1093/chromsci/6.10.501.

(18) Poole, C. F. *The Essence of Chromatography*, 1st ed.; Elsevier: Amsterdam ; Boston, 2003.

(19) Ghosh, A.; Johnson, J. E.; Nuss, J. G.; Stark, B. A.; Hawkins, A. R.; Tolley, L. T.; Iverson, B. D.; Tolley, H. D.; Lee, M. L. Extending the Upper Temperature Range of Gas Chromatography with All-Silicon Microchip Columns Using a Heater/Clamp Assembly. *J. Chromatogr. A* **2017**, *1517*, 134–141. DOI :10.1016/j.chroma.2017.08.036.

(20) Rotzsche, H. *Stationary Phases in Gas Chromatography*; Journal of chromatography library; Elsevier ; Distributors for the U.S. and Canada, Elsevier Science Pub. Co: Amsterdam ; New York : New York, NY, U.S.A, 1991.

(21) Azzouz, I.; Vial, J.; Thiébaut, D.; Haudebourg, R.; Danaie, K.; Sassiat, P.; Breviere, J. Review of Stationary Phases for Microelectromechanical Systems in Gas Chromatography: Feasibility and Separations. *Anal. Bioanal. Chem.* **2014**, *406* (4), 981–994. DOI :10.1007/s00216-013-7168-7.

(22) Gholizadeh, A.; Chowdhury, M.; Agah, M. Parallel Ionic Liquid Semi-Packed Microfabricated Columns for Complex Gas Analysis. *Anal. Chem.* **2020**, *92* (15), 10635–10642. DOI :10.1021/acs.analchem.0c01721.

(23) Gholizadeh, A.; Chowdhury, M.; Agah, M. Ionic Liquid Stationary Phase Coating Optimization for Semi-Packed Microfabricated Columns. *J. Chromatogr. A* **2021**, *1647*, 462144. DOI :10.1016/j.chroma.2021.462144.

(24) Regmi, B. P.; Chan, R.; Agah, M. Ionic Liquid Functionalization of Semi-Packed Columns for High-Performance Gas Chromatographic Separations. *J. Chromatogr. A* **2017**, *1510*, 66–72. DOI :10.1016/j.chroma.2017.06.050.

(25) Collin, W. R.; Bondy, A.; Paul, D.; Kurabayashi, K.; Zellers, E. T. MGC × MGC: Comprehensive Two-Dimensional Gas Chromatographic Separations with Microfabricated Components. *Anal. Chem.* **2015**, *87* (3), 1630–1637. DOI :10.1021/ac5032226.

(26) Dallüge, J.; Beens, J.; Brinkman, U. A. T. Comprehensive Two-Dimensional Gas Chromatography: A Powerful and Versatile Analytical Tool. *J. Chromatogr. A* **2003**, *1000* (1–2), 69–108. DOI :10.1016/S0021-9673(03)00242-5.

(27) Schoenmakers, P. J.; Oomen, J. L. M. M.; Blomberg, J.; Genuit, W.; van Velzen, G. Comparison of Comprehensive Two-Dimensional Gas Chromatography and Gas Chromatography – Mass Spectrometry for the Characterization of Complex Hydrocarbon Mixtures. *J. Chromatogr. A* **2000**, *892* (1–2), 29–46. DOI :10.1016/S0021-9673(00)00744-5.

(28) Giardina, M.; McCurry, J. D.; Cardinael, P.; Semard-Jousset, G.; Cordero, C.; Bicchi, C. Development and Validation of a Pneumatic Model for the Reversed-Flow Differential Flow Modulator for Comprehensive Two-Dimensional Gas Chromatography. *J. Chromatogr. A* **2018**, *1577*, 72–81. DOI :10.1016/j.chroma.2018.09.022.

(29) Delahousse, G.; Peulon-Agasse, V.; Debray, J.-C.; Vaccaro, M.; Cravotto, G.; Jabin, I.; Cardinael, P. The Incorporation of Calix[6]Arene and Cyclodextrin Derivatives into Sol–Gels for the Preparation of Stationary Phases for Gas Chromatography. *J. Chromatogr. A* **2013**, *1318*, 207–216. DOI :10.1016/j.chroma.2013.10.007.

(30) Burel, A.; Vaccaro, M.; Cartigny, Y.; Tisse, S.; Coquerel, G.; Cardinael, P. Retention Modeling and Retention Time Prediction in Gas Chromatography and Flow-Modulation Comprehensive Two-Dimensional Gas Chromatography: The Contribution of Pressure on Solute Partition. *J. Chromatogr. A* **2017**, *1485*, 101–119. DOI :10.1016/j.chroma.2017.01.011.

(31) Ghosh, A.; Bates, C. T.; Seeley, S. K.; Seeley, J. V. High Speed Deans Switch for Low Duty Cycle Comprehensive Two-Dimensional Gas Chromatography. *J. Chromatogr. A* **2013**, *1291*, 146–154. DOI :10.1016/j.chroma.2013.04.003.

(32) Tranchida, P. Q.; Maimone, M.; Franchina, F. A.; Bjerk, T. R.; Zini, C. A.; Purcaro, G.; Mondello, L. Four-Stage (Low-)Flow Modulation Comprehensive Gas Chromatography-quadrupole Mass Spectrometry for the Determination of Recently-Highlighted Cosmetic Allergens. *J. Chromatogr. A* **2016**, *1439*, 144–151. DOI :10.1016/j.chroma.2015.12.002.

(33) Schöneich, S.; Gough, D. V.; Trinklein, T. J.; Synovec, R. E. Dynamic Pressure Gradient Modulation for Comprehensive Two-Dimensional Gas Chromatography with Time-of-Flight Mass Spectrometry Detection. *J. Chromatogr. A* **2020**, *1620*, 460982. DOI :10.1016/j.chroma.2020.460982.

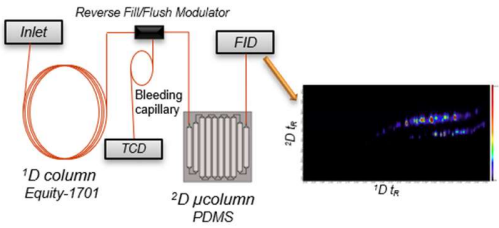
Reverse Fill/Flush Modulator
Inlet
FID
Bleeding capillary
TCD
^{1}D column
Equity-1701
^{2}D µcolumn
PDMS
^{2}D t_R
^{1}D t_R